ELSEVIER

Computers and Chemical Engineering 26 (2002) 1095–1102

Computers & Chemical Engineering

www.elsevier.com/locate/compchemeng

Drag reduction in flow over a flat plate using active feedback control

James Baker [a], James Myatt [b], Panagiotis D. Christofides [a,*]

[a] *Department of Chemical Engineering, University of California, 5531 Boelter Hall, 405 Hilgard Avenue, Los Angeles, CA 90095-1592, USA*
[b] *Air Force Research Lab/VACA, Wright Patterson Air Force Base, Dayton, OH 45433, USA*

Accepted 22 February 2002

Abstract

This paper focuses on two-dimensional incompressible Newtonian fluid flow over a flat plate and studies the problem of reducing the frictional drag exerted on the plate using active feedback control. Several alternative control configurations, including both pointwise and spatially uniform control actuation and sensing, are developed and tested through computer simulations. All control configurations use control actuation in the form of blowing/suction on the plate and measurements of shear stresses along the plate. The simulation results indicate that the use of active feedback control, which employs reasonable control effort, can significantly reduce the frictional drag exerted on the plate compared to the open-loop values.

Keywords: Distributed parameter systems; Flow control; Control actuation

1. Introduction

The problem of trying to influence a flow field to behave in a desirable way has received significant attention in the past (see e.g. Gad-el-Hak, 1994; Gad-el-Hak & Bushnell, 1991 for results in this area and reference lists). In general, fluid flow control can be classified in two categories: passive and active. Passive control typically involves some kind of design modification of the surface (e.g. wall-mounted, streamwise ribs or riblets) and requires no auxiliary power, while active control involves continuous adjustment of a variable that affects the flow based on measurements of quantities of the flow field (feedback). The approach of using active feedback control is particularly attractive as it enables drag reduction to occur by sensing and reacting to an unanticipated local flow state, as opposed to optimizing open-loop control actuation about a single, or multiple flow configurations.

Recent advances in manufacturing of control actuators (e.g. blowing/suction, synthetic jets, plasma-based electromagnetic forcing) and measurement sensors (e.g. shear stress sensors) make active feedback control of aerodynamic flows for frictional drag reduction and delay of separation a very real possibility. Within an open-loop control setting, several studies have shown that small devices with relatively little energy input can be extremely effective in influencing a flow field, motivating research interest on closed-loop feedback control of fluids. Over the last decade, several efforts have been made on the design and implementation of feedback control systems on various fluid flows. The approach followed for controller design typically involves the derivation of low-order ordinary differential equations (ODEs) approximations of the Navier–Stokes equations which describe the flow field using advanced discretization schemes including linear and nonlinear Galerkin's methods and reduced basis methods. These ODE systems are subsequently used for the design of low-order output feedback controllers. This approach has led to the design of robust optimal controllers for flow in a driven cavity (Burns & King, 1994; Burns & Ou, 1994; King & Qu, 1995), linear optimal and robust controllers for channel flow using boundary (blowing and suction) control actuation (Cortelezzi, Lee, Kim, & Speyer, 1998; Cortelezzi & Speyer, 1998; Joshi, Speyer,

* Corresponding author. Tel.: +1-310-794-1015; fax: +1-310-206-4107
E-mail address: pdc@seas.ucla.edu (P.D. Christofides).

0098-1354/02/$ - see front matter
PII: S0098-1354(02)00028-5

& Kim, 1995), linear controllers for flow over flat plate (Singh & Bandyopadhyav, 1997) and nonlinear controllers for channel flow (Baker, Armaou, & Christofides, 2000) using distributed (electromagnetic forcing) control actuation, and linear and nonlinear controllers for suppression of wavy behavior exhibited by fluid dynamic systems described by the Korteweg-de Vries-Burgers (Armaou & Christofides, 2000b) and Kuramoto–Sivashinsky (Armaou & Christofides, 2000a,b; Christofides & Armaou, 2000) equations. An alternative approach to controller design is based on the concept of designing a feedback controller so that the time-derivative of an appropriate Lyapunov functional along the trajectories of the closed-loop system is negative definite and has been used to design controllers for the channel flow (Balogh, Liu, & Krstić, 2001; Kang & Ito, 1992), and the Kuramoto–Sivashinsky (Liu & Krstić, 2001) equation. Other results include the solution of the optimal control problem for the Navier–Stokes equations with distributed control (Desai & Ito, 1994; Hou & Yan, 1997) and proportional–integral control (Beringen, 1984; Choi, Moin, & Kim, 1994; Choi, Temam, Mom, & Kim, 1993; Joshi, Speyer, & Kim, 1997).

In this work, we focus on a two-dimensional incompressible Newtonian fluid flow over a flat plate (Fig. 1) and consider the problem of reducing the frictional drag exerted on the plate using active feedback control. Several alternative control configurations, including both pointwise and spatially uniform control actuation and sensing, are developed and tested through computer simulations. All control configurations use control actuation in the form of blowing/suction on the plate and measurements of shear stresses along the plate. The simulation results indicate that the use of active feedback control, which employs reasonable control effort, can significantly reduce the frictional drag exerted on the plate compared to the open-loop values.

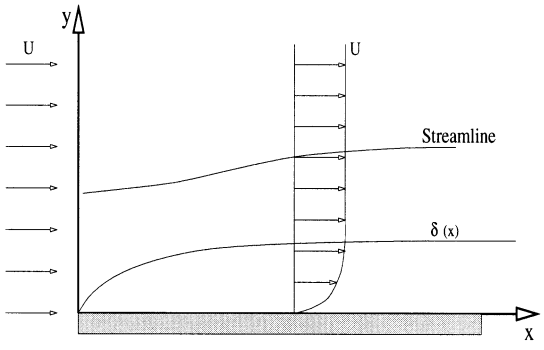

Fig. 1. Flow over a flat plate.

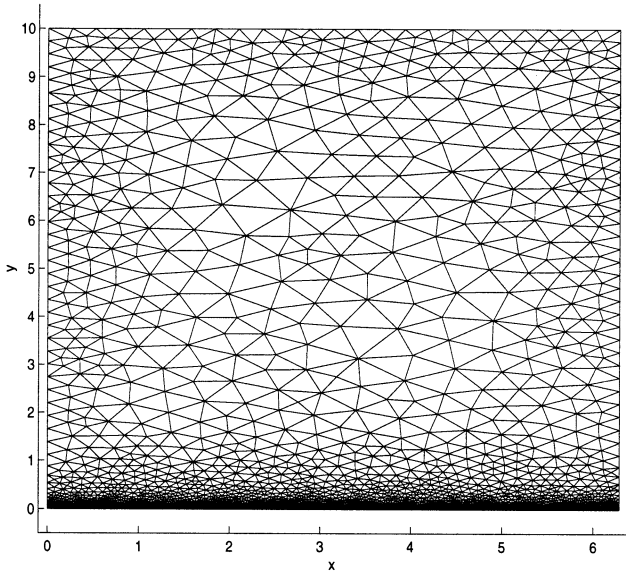

Fig. 2. Spatial domain and finite-element mesh for flow over a flat plate.

2. Flow field equations

We consider a two-dimensional incompressible Newtonian fluid flow with uniform velocity, which is equal to a constant U_0, over a flat plate of length L. The exact dimensions of the rectangular domain used for this fluid dynamic system and the (x, y) axes specification used in all of our calculations are shown in (Fig. 2). Owing to symmetry, only one half (the upper half) of the geometry is generated. The Navier–Stokes equations that describe the flow field take the following form:

$$\frac{\partial u}{\partial x}+\frac{\partial v}{\partial y}=0$$

$$\frac{\partial u}{\partial t}+u\frac{\partial u}{\partial x}+v\frac{\partial u}{\partial y}=-\frac{1}{\rho}\frac{\partial P}{\partial x}+\nu\frac{\partial^2 u}{\partial x^2}+\nu\frac{\partial^2 u}{\partial y^2}$$

$$\frac{\partial v}{\partial t}+u\frac{\partial v}{\partial x}+v\frac{\partial v}{\partial y}=-\frac{1}{\rho}\frac{\partial P}{\partial y}+\nu\frac{\partial^2 v}{\partial x^2}+\nu\frac{\partial^2 v}{\partial y^2} \quad (1)$$

where u and v are the components of the velocity along the x and y axes, respectively, P is the pressure, ρ is the fluid density, and ν is the kinematic viscosity. The above equations were considered subject to the following set of boundary conditions:

$$u(0, y, t)=U_0, \quad v(0, y, t)=0$$

$$u(x, 0, t)=0, \quad v(x, 0, t)=C(x, t)$$

$$n_x u(x, 10, t)+n_y v(x, 10, t)=0 \quad (2)$$

where $C(x, t)$ is the control input that will be determined in the next section and (n_x, n_y) are the components of the vector normal to the boundary (i.e. $n=n_x i+n_y j$). Note that the fact that we set $v(x, 0, t)=C(x, t)$ is motivated by our desire to control the flow using vertical blowing/suction. For the open-loop

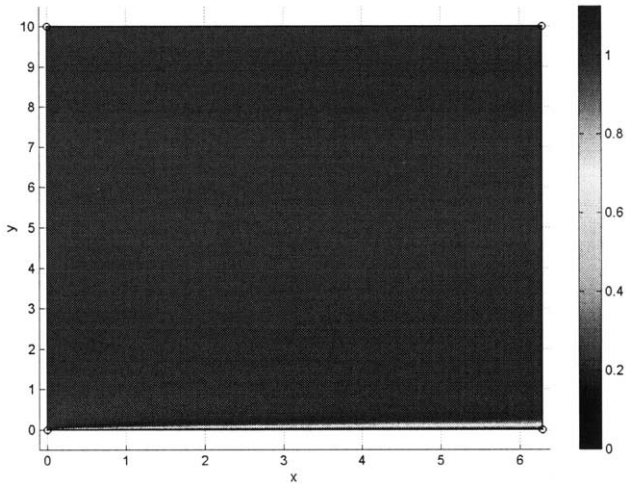

Fig. 3. Steady-state open-loop velocity profile for flow over flat plate for the entire domain.

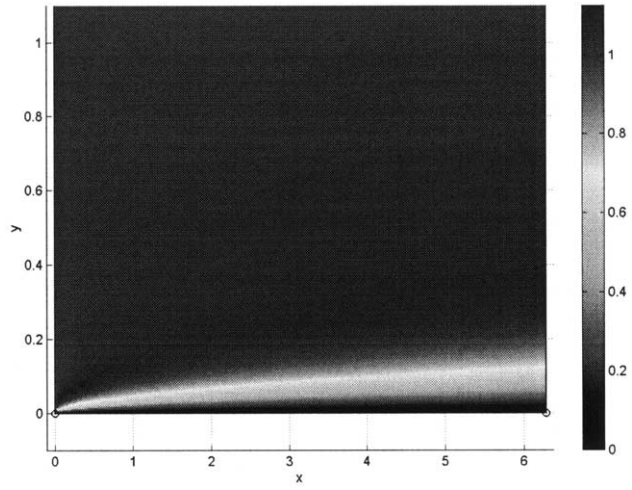

Fig. 4. Steady-state open-loop velocity profile for flow over flat plate close to the plate.

system (i.e. $C(x, t) = 0$), the first two boundary conditions imply that the flow towards the plate is uniform, the next two boundary conditions correspond to no-slip on the plate, and the last boundary condition accounts for the fact that far from the plate the flow should be uniform. In addition, since the profile of the flow in the outlet of the plate is unknown, following (Papanastasiou, Malamataris, & Ellwood, 1992; Renardy, 1997) a free boundary condition was employed in the outlet and the outlet pressure $P(6.3, y)$ was set equal to one.

We developed a program within the FEMLAB simulation environment that uses a finite element approach with a very fine mesh to compute the solution of the flow field as described by the dynamic Navier–Stokes of Eqs. (6)–(8); further increase in the number of discretization elements and decrease of the step of the temporal integration did not influence the results. The exact form of the spatial discretization mesh used in our calculations for both the open-loop and the closed-loop system is shown in Fig. 2. It is important to note that the finer structure of the mesh towards the plate was motivated by the presence of the plate which leads to significant velocity gradients close to the plate and of our closed-loop calculations (to be presented in the next section) that require a finer mesh close to the area where feedback control is applied to the system to maintain a mesh-independent solution. The last requirement is a result of the modification of the value of $C(x, t)$ from 0 for the open-loop system to an expression that is a function of the state of the system in the case of the closed-loop system. To be able to make meaningful comparisons for the frictional drag profiles along the plate, we used the same mesh structure for the open-loop and closed-loop simulations. Moreover, the height of the computational domain was taken to be about 30 times the thickness of the boundary layer (Fig. 3) to remove boundary effects to and ensure quick convergence and accuracy of the solution.

Figs. 3 and 4 show the steady-state open-loop velocity (each point in the plot represents the value of $\sqrt{u^2 + v^2}$) profiles for the entire domain and close to the plate, respectively, for $Re = 50\,000$ (where $\mathrm{Re} = \mathrm{Vol}/v$ is the Reynolds number); we can see the development of a laminar boundary layer over the plate. This is expected since for $Re = 50\,000$ the boundary layer over the plate is stable (Batchelor, 1967, page 313). The reason for which the time axis starts from 30 time units is that it takes 30 time units for the flow to stabilize at the laminar boundary layer configuration; this time axis specification will facilitate the comparisons between the open-loop and closed-loop system drag profiles. The computation of the pressure gradients $\partial P/\partial x$ and $\partial P/\partial y$ gave very small values for these two quantities everywhere in the flow field; this is expected in the case of uniform external flow (see also Remark 3). Furthermore, owing to the very fine mesh used in our calculations, the velocity close to the inlet was found to be uniform and equal to U_0 (except from the plate where it is zero), thereby eliminating the need to expand the computational domain to some small distance before the leading edge of the plate to achieve uniform flow in the inlet of the computational domain.

Since the objective of this work is to investigate the effect of feedback control (i.e. different choices for $C(x, t)$) on the frictional drag exerted on the plate (i.e. integral along x of the tangential force per unit area exerted on the plate by the fluid), we will present our results in terms of the quantity $\partial u/\partial y$ at $y = 0$ which is directly proportional to the frictional drag; the drag exerted on the two sides of unit width of a plate of length L is

$$D = 2\int_0^L \mu\left(\frac{\partial u}{\partial y}\right)_{y=0} \mathrm{d}x \tag{3}$$

Fig. 5 shows the spatio-temporal profile of $\partial u/\partial y$ at $y = 0$, over a flat plate for the open-loop (i.e. $C(x, t) = 0$) steady-state flow field. As expected for steady-state laminar boundary layer, $(\partial u/\partial y)_{y=0}$ exhibits its maximum close to the edge of the plate (see Remark 3 for a detailed discussion on this issue).

Remark 1. Owing to the consideration of an external flow field with $U = U_0 =$ constant, the possibility of separation of the flow from the plate at a certain position downstream does not exist. Flow separation can occur when the external flow accelerates/decelerates; active feedback control of flow separation is a subject currently studied by our group but it is outside of the scope of the present paper.

Remark 2. We also verified that the use of the boundary condition $u(x, 10, t) = U_0, \quad v(x, 10, t) = 0$ on the top side of the computational domain leads to identical results to the ones of the slip boundary condition, $n_x u(x, 10, t) + n_y v(x, 10, t) = 0$ used in the calculations reported in the present paper. This is a consequence of the fact that the height of the computational domain is much larger than the thickness of the boundary layer.

Remark 3. The objective of this remark is to review the approximate steady-state boundary layer equations for laminar flow over flat plate and provide the resulting analytic expression of the frictional drag per unit area of the plate at distance x from the leading edge (the reader may refer to Batchelor, 1967 for more discussion on this subject). To proceed with this task, we first evaluate the pressure gradient $\partial P/\partial x$ outside of the boundary layer. At the edge of the boundary layer using Euler's equation for the incident irrotational flow and using a no-penetration condition, we obtain:

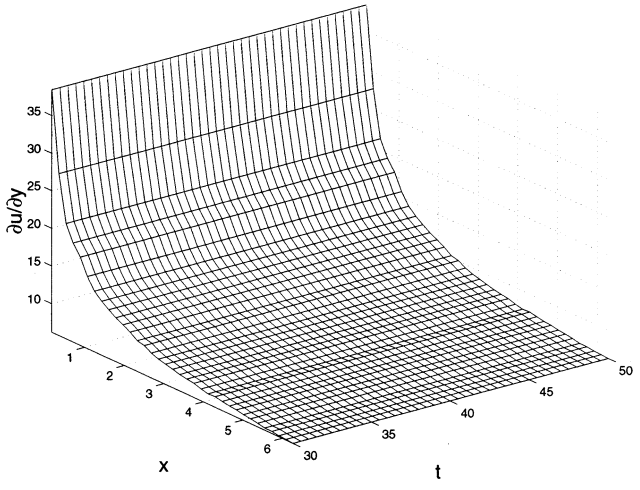

Fig. 5. Spatio-temporal profile of $(\partial u/\partial y)_{y=0}$ for $C(x, t) = 0$.

$$-\frac{1}{\rho}\frac{\partial P}{\partial x} = \frac{\partial U}{\partial t} + U\frac{\partial U}{\partial x} \tag{4}$$

where U represents the known tangential component of the velocity of the outer flow. For uniform flow outside of the boundary layer, it follows directly from Eq. (4) that $U = U_0$ implies $\partial P/\partial x = 0$.

To proceed with the derivation of the approximate steady-state boundary layer equations, we need to obtain a more natural coordinate system in which lateral distances are measured and velocities are measured with the (representative) boundary layer thickness as the unit length; this will allow to state clearly the main assumptions involved in this approximation. To this end, we define the following dimensionless quantities:

$$\bar{x} = \frac{x}{L}, \quad \bar{y} = Re^{0.5}\frac{y}{L}, \quad \bar{t} = \frac{tU_0}{L},$$

$$\bar{u} = \frac{u}{U_0}, \quad \bar{v} = Re^{0.5}\frac{v}{U_0}, \quad \bar{P} = \frac{P - P_0}{\rho U_0^2} \tag{5}$$

where L represents a distance in the x-direction over which u changes appreciably and P_0 is the value of P at some convenient reference point in the fluid. Using these new variables, the Navier–Stokes equations of Eq. (1) with $\partial\bar{P}/\partial\bar{x} = 0$ that describe the flow field take the form:

$$\frac{\partial\bar{u}}{\partial\bar{x}} + \frac{\partial\bar{v}}{\partial\bar{y}} = 0$$

$$\frac{\partial\bar{u}}{\partial\bar{t}} + \bar{u}\frac{\partial\bar{u}}{\partial\bar{x}} + \bar{v}\frac{\partial\bar{u}}{\partial\bar{y}} = \frac{1}{Re}\frac{\partial^2\bar{u}}{\partial\bar{x}^2} + \frac{\partial^2\bar{u}}{\partial\bar{y}^2}$$

$$\frac{1}{Re}\left(\frac{\partial\bar{v}}{\partial\bar{t}} + \bar{u}\frac{\partial\bar{v}}{\partial\bar{x}} + \bar{v}\frac{\partial\bar{v}}{\partial\bar{y}}\right) = -\frac{\partial\bar{P}}{\partial\bar{y}} + \frac{1}{Re^2}\frac{\partial^2\bar{v}}{\partial\bar{x}^2} + \frac{1}{Re}\frac{\partial^2\bar{v}}{\partial\bar{y}^2} \tag{6}$$

The approximate steady-state laminar boundary layer equations can be obtained under the assumptions that $Re \to \infty$ and the magnitude of $\partial u/\partial x$ is small compared with that of $\partial u/\partial y$ and have the form:

$$\frac{\partial\bar{u}}{\partial\bar{x}} + \frac{\partial\bar{v}}{\partial\bar{y}} = 0$$

$$\bar{u}\frac{\partial\bar{u}}{\partial\bar{x}} + \bar{v}\frac{\partial\bar{v}}{\partial\bar{y}} = \frac{\partial^2\bar{u}}{\partial\bar{y}^2}, \qquad 0 = -\frac{\partial\bar{P}}{\partial\bar{y}} \tag{7}$$

The above equations are subjected to the following set of boundary conditions:

$$\bar{u}(\bar{x}, 0, \bar{t}) = 0, \quad \bar{v}(\bar{x}, 0, \bar{t}) = \bar{C}(\bar{x},\bar{t})$$

$$\bar{u}(\bar{x}, 0, \bar{t}) \to 1 \qquad \text{as } \frac{\bar{y}}{\delta_0} \to \infty \tag{8}$$

where δ_0 is a small length representative of the boundary layer thickness. The solution of Eqs. (7) and (8) can be obtained with appropriate similarity transformations and leads to the following expression for the frictional force per unit area of the plate (expressed in terms of the original coordinates) at distance x from the leading edge (Batchelor, 1967):

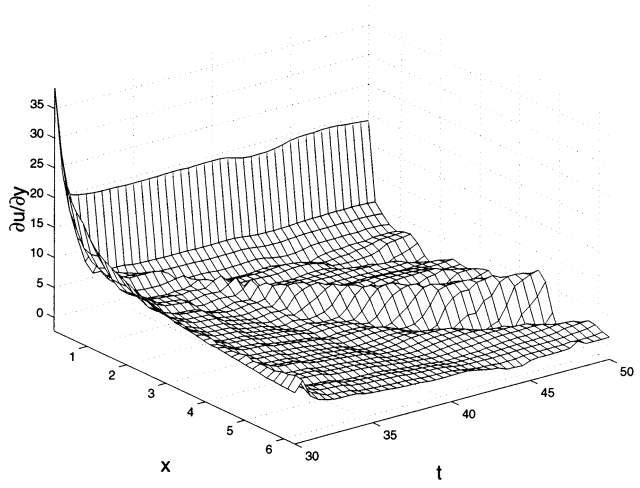

Fig. 6. Spatio-temporal profile of $(\partial u/\partial y)_{y=0}$ for the case of collocated actuator/sensor control configuration.

$$\mu\left(\frac{\partial u}{\partial y}\right)_{y=0} = 0.33\rho U_0^2 Re^{-0.5}\left(\frac{x}{L}\right)^{-0.5} \tag{9}$$

which clearly implies that $(\partial u/\partial y)_{y=0}$ attains its maximum at the leading edge of the plate and decreases to zero as x increases. Note that the calculation of the frictional drag of Eq. (9) is not valid if the flow in the boundary layer is not laminar (unstable flow occurs for Re greater than 1.2×10^5 (Batchelor, 1967, page 313) which is significantly above the value of $Re=5\times10^4$ considered in our simulations) over the whole surface of the flat plate. In the case of unstable flow, disturbances in the boundary layer grow and a transition to a different type of flow occurs at some distance downstream. The frictional force at the wall in such a turbulent boundary layer is considerably larger than that in a laminar boundary layer with the same external stream speed, because the random cross-currents in the boundary layer carry the fast moving fluid in the outer layers into the neighborhood of the wall and are more effective in promoting lateral transport than molecular diffusion.

3. Control laws—closed-loop simulations

We developed several alternative control configurations (i.e. different actuation/measurement structures) which use wall shear stress measurements and apply blowing/suction type of control actuation to reduce the frictional drag exerted on the plate. All control configurations utilize linear proportional control laws to compute the control action. More specifically, in the case of pointwise measurement/actuation, the control law is of the type $C(x_i,t)=K(\partial u/\partial y)(x_i,0,t)$, where K is the controller gain and x_i is the location of actuation, while in the case of spatially uniform control actuation, the control law is of the type $C(t)=K\int_0^L s(x)(\partial u/\partial y)(x,0,t)\mathrm{d}x$, where $s(x)$ is a function which depends on the type of measurements (pointwise, distributed) that are available for feedback. The simple structure of the above feedback laws is motivated by the following three reasons: (a) the objective of this study is to see whether it is possible to reduce frictional drag with any type (in particular the simplest) of active feedback control, (b) the design of Navier–Stokes-based feedback controls is not an easy task owing to the complexity of the flow field under consideration, while the on-line implementation of such controls would require significant computational power which may not always be available, and (c) the practical implementation of the above linear control laws requires relatively less computational and hardware resources. The value of the controller gain K was chosen, through trial and error, to achieve a reasonable reduction in frictional drag and to avoid perturbing the laminar nature of the flow field in the domain of definition of the flow. In all the simulation runs discussed below, $Re=50\,000$.

We initially tested a fully localized control configuration which uses the value of the wall shear stress at any given point along the plate to determine the amount of blowing/suction (i.e. value of the vertical component of the velocity) at the corresponding point on the plate. Mathematically, the control law for this case can be expressed as:

$$v(x_i,0,t)=C(x_i,t)=K\left(\frac{\partial u}{\partial y}\right)(x_i,0,t), \qquad i=1,\ldots,N \tag{10}$$

where $K=0.005$ and $N=350$ is the number of discretization points used on the plate.

Fig. 6 shows the spatio-temporal profile of $(\partial u/\partial y)_{y=0}$ starting from initial conditions of the steady-state open-loop simulation. Again as in the open-loop simulations, the time axis starts from 30 time units; this is the time needed for the flow to reach the steady-state solution of the open-loop system and $t=30$ is the time in which we activate the control system. As can be seen in Fig. 6, this control configuration does a very good job in reducing the frictional drag compared to the open-loop operation (compare the profile of Fig. 6 with the corresponding open-loop profile of Fig. 5). Fig. 7 shows the spatio-temporal profile of the wall-normal velocity, $v(x,0,t)$, which is the manipulated input. Clearly, the value of $v(x,0,t)$ is small and positive for all times which means that blowing is applied to the flow. Note also that, as expected in the case of collocated actuation/sensing (control input at each point depends only on the measurement at the same point), the profile of $v(x,0,t)$ is not uniform along x.

We also tested several alternative control configurations. Specifically, we considered a control configuration which uses the average of five equally spaced point

measurements of $(\partial u/\partial y)_{y=0}$ on the flat plate to apply spatially uniform control actuation, that is:

$$v(x, 0, t) = C(t) = \frac{K}{5}\sum_{i=1}^{5}\left(\frac{\partial u}{\partial y}\right)(x_i, 0, t) \quad (11)$$

where $K = 0.005$. The above control law can be derived from the general integral feedback control structure presented in the beginning of this section by setting $s(x) = 1/5\Sigma_{i=1}^{5}\delta(x - x_i)$, where $\delta(\cdot)$ is the standard Dirac function. Fig. 8 shows the spatio-temporal profile of $(\partial u/\partial y)_{y=0}$ starting from initial conditions of the steady-state open-loop simulation. This control configuration does a very good job in reducing the frictional drag compared to the open-loop operation. Fig. 9 shows the spatio-temporal profile of the wall-normal velocity, $v(x, 0, t)$, which is the manipulated input. Clearly the value of $v(x, 0, t)$ is small and positive for all times which means that blowing is applied to the flow. Note also that, as expected in the case of spatially uniform control actuation, the profile of $v(x, 0, t)$ is uniform along x.

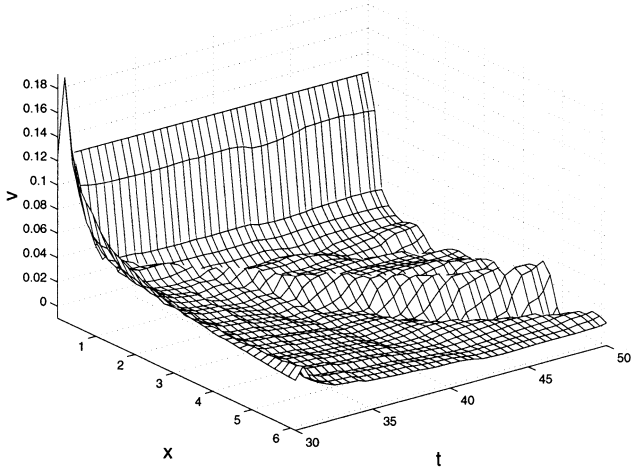

Fig. 7. Spatio-temporal profile of the wall-normal velocity, $v(x, 0, t)$, for the case of collocated actuator/sensor control configuration.

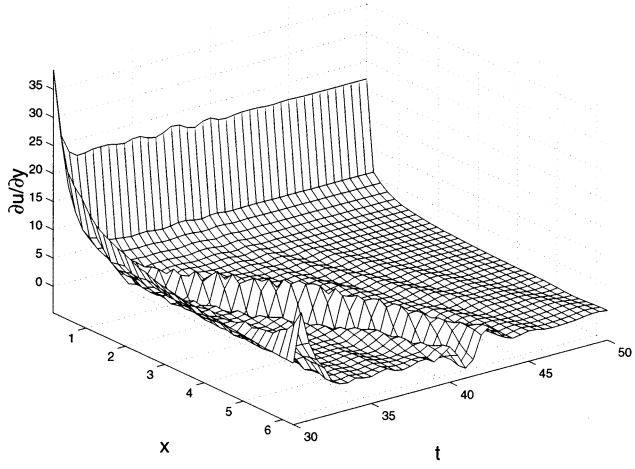

Fig. 8. Spatio-temporal profile of $(\partial u/\partial y)_{y=0}$ for the case of spatially uniform control actuation with five equally spaced point measurements.

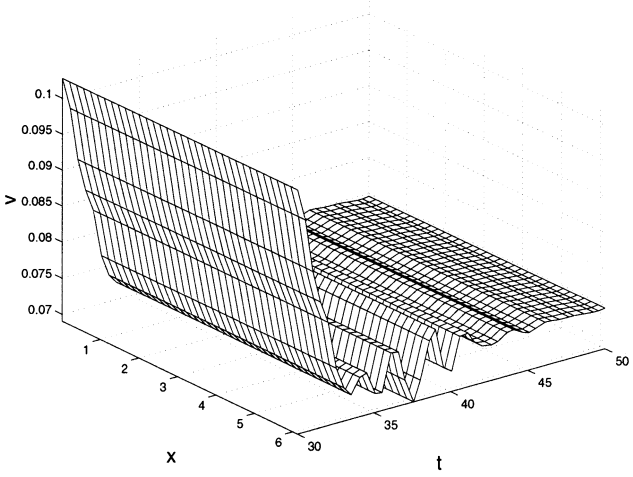

Fig. 9. Spatio-temporal profile of the wall-normal velocity, $v(x, 0, t)$, for the case of spatially uniform control actuation with five equally spaced point measurements (the first measurement is taken at the leading edge of the plate).

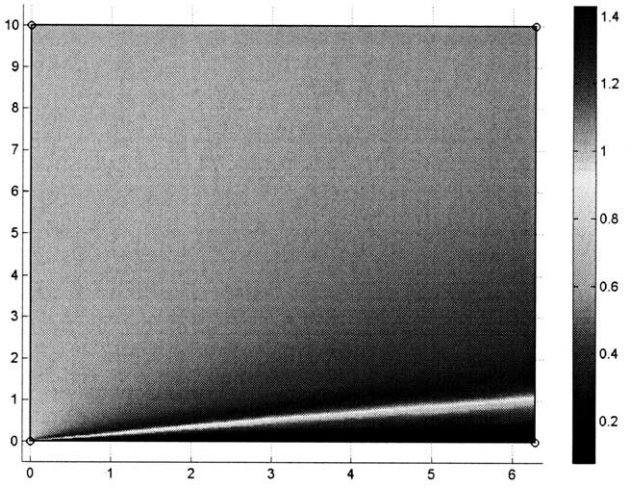

Fig. 10. Steady-state closed-loop velocity profile for flow over flat plate for the entire domain, for the case of spatially uniform control actuation with five equally spaced point measurements.

Fig. 10 shows the corresponding velocity profile for the entire domain, respectively; the use of blowing on the plate slows down the flow very close to the plate, thereby reducing the frictional drag on the plate and increasing the value of the velocity field close to the edge of the boundary layer compared to the open-loop velocity of Fig. 3 (see also Fig. 4). We also tested the robustness of the control scheme of Eq. (11) with respect to a sinusoidal profile of amplitude 0.1 which was superimposed on the calculated average of the five measurements to simulate a time-varying disturbance in

the measurements. Fig. 11 shows the spatio-temporal profile of $(\partial u/\partial y)_{y=0}$ starting from initial conditions of the steady-state open-loop simulation and Fig. 12 shows the spatio-temporal profile of $v(x, 0, t)$ for this simulation run. While the disturbance influences the flow, the controller is capable of reducing the value of $(\partial u/\partial y)_{y=0}$ below the open-loop level using blowing. Note also that owing to the persistent nature of the disturbance, the profile of $v(x, 0, t)$ exhibits a slight variation with respect to time for large times (this is not the case in the profile of $v(x, 0, t)$ in the previous simulation run, Fig. 9, where disturbances have not been included).

Finally, we developed and tested a control configuration which uses the average of many point measurements of $\partial u/\partial y$ on the flat plate to calculate the spatially uniform control actuation applied to the flow field along the plate; this was done to evaluate the effect of the number and location of measurements on controller performance (amount of control action) and closed-loop performance (frictional drag reduction).

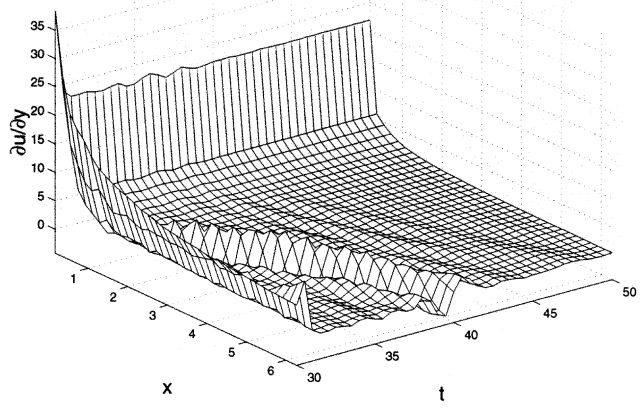

Fig. 11. Spatio-temporal profile of $(\partial u/\partial y)_{y=0}$ for the case of spatially uniform control actuation with five equally spaced point measurements; robustness with respect to measurement disturbances.

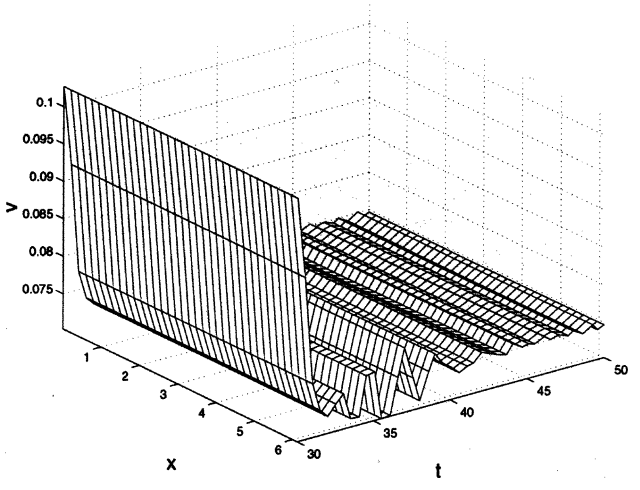

Fig. 12. Spatio-temporal profile of the wall-normal velocity, $v(x, 0, t)$, for the case of spatially uniform control actuation with five equally spaced point measurements; robustness with respect to measurement disturbances.

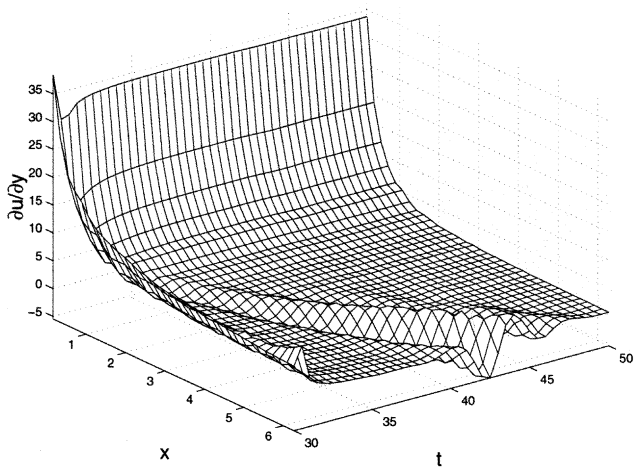

Fig. 13. Spatio-temporal profile of $(\partial u/\partial y)_{y=0}$ for the case of spatially uniform control actuation with 350 equally spaced point measurements.

In this case, the control law has the following form:

$$v(x,0,t) = C(t) = \frac{K}{N}\sum_{i=1}^{N}\left(\frac{\partial u}{\partial y}\right)(x_i, 0, t) \tag{12}$$

where $K = 0.005$ and $N = 350$. The above control law can be also derived from the general integral feedback control structure presented in the beginning of this section by setting $s(x) = \frac{1}{N}\Sigma_{i=1}^{N}\delta(x - x_i)$.

Fig. 13 shows the spatio-temporal profile of $(\partial u/\partial y)_{y=0}$ starting from initial conditions of the steady-state open-loop simulation and Fig. 14 shows the spatio-temporal profile of $v(x, 0, t)$ for this simulation run. While this control configuration reduces the frictional drag compared to the open-loop system using blowing, it does not provide a significant improvement (in terms of reduction of the frictional drag) compared to the closed-loop performance achieved with the control configuration of Eq. (11) which uses only five measurements of $(\partial u/\partial y)_{y=0}$. However, the advantage of using a large number of measurements can be seen by studying the input profile of Fig. 14 and comparing it with the input profile of Fig. 9. Clearly, the use of a large number of measurements taken at spatial locations that are not close to the edge of the plate (where $(\partial u/\partial y)_{y=0}$ attains its maximum value for both the open- and closed-loop systems) leads to a substantially smaller control action and a smoother control input profile; thereby improving the robustness of the laminar closed-loop flow field with respect to disturbances and transition to turbulence.

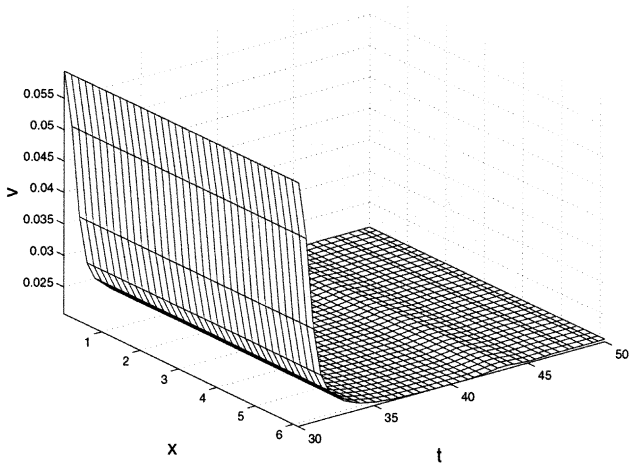

Fig. 14. Spatio-temporal profile of the wall-normal velocity, $v(x, 0, t)$, for the case of spatially uniform control actuation with 350 equally spaced point measurements.

The main conclusion of the present simulation study is that the use of active feedback control, which employs reasonable control effort, can significantly reduce the frictional drag exerted on the plate compared to the open-loop values. Furthermore, our results suggest that: (a) a small number of measurement sensors may be sufficient to achieve drag reduction, and (b) the measurement sensor and control actuator locations can significantly influence flow dynamics and controller performance and should be carefully chosen to avoid using unnecessarily large control action. Further work will be needed to check the robustness of these results with respect to variations of the Reynolds number and examine the derivation of flow models suitable for model-based controller design and implementation.

References

Armaou, A., & Christofides, P. D. (2000a). Feedback control of the Kuramoto–Sivashinsky equation. *Physica D*, *137*, 49–61.

Armaou, A., & Christofides, P. D. (2000b). Wave suppression by nonlinear finite-dimensional control. *Chemical Engineering and Science*, *55*, 2627–2640.

Baker, J., Armaou, A., & Christofides, P. D. (2000). Nonlinear control of incompressible fluid flow: Application to Burgers equation and 2D channel flow. *J. Math. Anal. Appl.*, *252*, 230–255.

Balogh, A., Liu, W.-J., & Krstić, M. (2001). Stability-enhancement by boundary control in 2D channel flow. *IEEE Transactions on Automatic Control*, *46*, 1696–1711.

Batchelor, G. K. (1967). *An introduction to fluid dynamics*. Great Britain: Cambridge University Press, Cambridge.

Beringen, S. (1984). Active control of transition by periodic suction and blowing. *Physics and Fluids*, *27*, 1345–1348.

Burns, J.A., King, B.B. (1994). Optimal sensor location for robust control of distributed parameter systems. *Proceedings of thirtythird IEEE Conference on Decision and Control* (pp. 3965–3970). Orlando, FL.

Burns, J.A., Ou, Y.-R. (1994). Feedback control of the driven cavity problem using LQR designs. *Proceedings of thirtythird IEEE Conference on Decision and Control* (pp. 289–294). Orlando, FL.

Choi, H., Moin, P., & Kim, J. (1994). Active turbulence control for drag reduction in wall-bounded flows. *Journal of Fluid Mechanics*, *262*, 75–110.

Choi, H., Temam, R., Mom, P., & Kim, J. (1993). Feedback control for unsteady flow and its application to the stochastic Burger's equation. *Journal of Fluid Mechanics*, *253*, 509–543.

Christofides, P. D., & Armaou, A. (2000). Global stabilization of the Kuramoto–Sivashinsky equation via distributed output feedback control. *Systems and Control Letters*, *39*, 283–294.

Cortelezzi, L., Lee, K. H., Kim, J., & Speyer, J. L. (1998). Skin-friction drag reduction via reduced-order linear feedback control. *International Journal of Computational Fluid Dynamics*, *11*, 79–92.

Cortelezzi, L., & Speyer, J. L. (1998). Robust reduced-order controller of laminar boundary layer transition. *Rhys. Review E*, *58*, 1906–1910.

Desai, M., & Ito, K. (1994). Optimal controls of Navier–Stokes equations. *SIAM Journal of Control and Optimization*, *32*, 1428–1446.

Gad-el-Hak, M. (1994). Interactive control of turbulent boundary layers: a futuristic overview. *AIAA Journal*, *32*, 17531765.

Gad-el-Hak, M., & Bushnell, D. M. (1991). Separation control. *Journal of Fluids Engineering*, *113*, 5–30.

Hou, L. S., & Yan, Y. (1997). Dynamics for controlled Navier–Stokes systems with distributed controls. *SIAM Journal of Control and Optimization*, *35*, 654–677.

Joshi, S.S., Speyer, J.L., Kim, J. (1995). Modeling and control of two dimensional poiseuille flow. *Proceedings of thirtyfourth IEEE Conference on Decision and Control* (pp. 921–927). New Orleans, LA.

Joshi, S. S., Speyer, J. L., & Kim, J. (1997). A system theory approach to the feedback stabilization of infinitesimal and finite-amplitude disturbances in plane Poiseuille flows. *Journal of Fluid Mechanics*, *332*, 157–184.

Kang, S., Ito, K. (1992). A feedback control law, for systems arising in fluid dynamics. *Proceedings of thirtieth IEEE Conference on Decision and Control* (pp. 384–385). Tampa, AZ.

King, B.B., Qu, Y. (1995). Nonlinear dynamic compensator design for flow control in a driven cavity. *Proceedings of thirtyfourth IEEE Conference on Decision and Control* (pp. 3741–3746). New Orleans, LA.

Liu, W.-J., & Krstić, M. (2001). Stability enhancement by boundary control in the Kuramoto–Sh ashinsky equation. *Nonlinear Analysis: Theory, Methods and Applications*, *43*, 485–507.

Papanastasiou, T. C., Malamataris, N., & Ellwood, K. (1992). A new outflow boundary condition. *International Journal of Numerical Methods in Fluids*, *14*, 587–608.

Renardy, M. (1997). Imposing 'no' boundary condition at outflow: why does it work? *International Journal of Numerical Methods in Fluids*, *24*, 413–417.

Singh, S. N., & Bandyopadhyav, P. R. (1997). Linear feedback control of boundary layer using electromagnetic microtiles. *Transactions of the ASME*, *119*, 852–858.